Journal of Fluids and Structures (2002) **16**(6), 761–772
doi:10.1006/jfls.450. available online at http://www.idealibrary.com on IDEAL®

UNSTEADY LIFT PRODUCED BY A STREAMWISE VORTEX IMPINGING ON AN AIRFOIL

M. S. Howe

*College of Engineering, Boston University, 110 Cummington Street
Boston MA 02215, USA*

(Received 20 December 2000; and in final form 1 November 2001)

An analytical model is investigated to estimate the spectrum of the unsteady lift produced by a low Mach number, streamwise vortex "playing" on the leading edge of a thin airfoil. The vortex is assumed to exhibit a random wave-like behavior induced by mean flow turbulence and upstream influence from the edge, and to contain quasi-periodic structures associated with its mode of generation at some upstream station at an appropriate 'shedding' Strouhal number. To calculate the resulting modulation of the lift, the quasi-periodic structures are modelled by a succession of uncorrelated vortex rings that impinge randomly on the leading edge within a bounded region determined by the mean flow conditions. The overall lift fluctuation can be calculated as a linear superposition of the separate lifts induced by each vortex, and this is used to evaluate the lift spectrum. The spectrum is broadband and relatively flat up to a maximum frequency determined by the vortex core diameter. This broadband region can typically span an interval of airfoil-reduced frequencies between 1 and 10^2.

1. INTRODUCTION

We Consider the problem of estimating the frequency spectrum of the unsteady lift produced when a streamwise oriented vortex in a low Mach number mean stream impinges on the nose of a thin airfoil. This can occur, for example, in a turbomachine, where rotor blades are often joined at their tips by a "shroud" designed to reduce noise and blade vibration. When a vortex shed from an upstream structural protuberance or blade tip, etc., reaches the shroud, it can pass between the shroud and the turbomachine casing, be ingested by the rotor, or develop in a much more complicated manner after being "cut" by the shroud leading edge. Related problems have been investigated experimentally, for example in connection with helicopter blade–vortex interactions (Wittmer *et al*. 1995; 1999; Wittmer & Devenport 1999), and the buffeting of tail fins by an impinging vortex (Mayori & Rockwell 1994; Wolfe *et al*. 1995; Canbazoglu *et al*. 1995). The reader is referred to the review by Rockwell (1998) of these and other related problems. All of these events result in an unsteady lift force on the shroud, normal to the casing, which in turn produces an essentially equal radial force on the casing, and is a possible source of vibration and sound (Curle 1955; Howe 1998).

The production of sound by vortex ingestion, where the vortex is "chopped" by the rotor blades, has been investigated theoretically by Howe (1988, 1991). Extension has been made by the author (Howe 2001) to examine the lift and sound generated by turbulence in the mean flow impinging on a shroud adjacent to a wall. The problem discussed in this

0889-9746/02/060761 + 12 $35.00/0

paper concerns a particular inflow disturbance consisting of a discrete vortex, nominally aligned with the mean flow direction into the shroud, but subject to random and quasi-periodic distortions, such that the vortex axis might be said to resemble, say, a helix of randomly variable pitch. Flows of this type are often associated with some sort of vortex breakdown just upstream of the airfoil (Wolfe *et al.* 1995; Rockwell 1998); the resulting vortex motion past the airfoil exhibits large undulations at a predominant "center frequency" that characterizes the dominant frequency of the unsteady surface loading for a wide range of Reynolds and Mach numbers. For a free-field airfoil, the broken down vortex typically splits into two, each part passing the airfoil on opposite sides, but the details of the actual flow depend critically on upstream conditions. In an actual flow it is probably more reasonable to regard these conditions as stochastic: the shape of the vortex is unknown, and subject to many random distortions produced by upstream influence of the shroud and variations in the background mean flow.

In the undisturbed state, the vortex core might ideally be approximated by a circular cylindrical region of streamwise vorticity. In a first approximation, when the flow speed is sufficiently large that vorticity may be assumed to convect passively in the mean stream [the usual approximation of "thin-airfoil–gust" interaction theory (Sears 1941; Gebert & Atassi 1989; Howe 2001)], streamwise orientated vorticity produces no lift on a shroud aligned with the flow. Lift fluctuations are generated primarily by the interaction of the *spanwise* component of gust vorticity with the shroud. In practice, discrete vortex structures tend to be released from bluff bodies, etc., quasi-periodically at some preferred *Strouhal* number $f_0 D/U$, where D is a pertinent dimension of the shedding body, U is the mean flow speed, and f_0 is the characteristic shedding frequency (Blevins 1977). This produces spatial and temporal variations in the shed vorticity that typically cause the vortex core to spiral around a streamwise path (Blevins 1977; Green 1995; Waitz *et al.* 1995). Random distortions induced by the flow result in changes in the vortex that tend to be correlated only over finite streamwise distances; the interaction of the vortex with the shroud should therefore be more properly regarded as a succession of uncorrelated interactions of quasi-periodic distinct vortex structures. A lift spectrum that might have been expected to be dominated by one or more spectral peaks associated with an ideal, deterministic inflow core geometry accordingly turns out to be broadband. The overall lift spectrum is determined by the average spectrum of the lift produced by the uncorrelated structures. This is entirely analogous to the quasi-periodic shedding mechanism that appears to control the spectrum of the unsteady side force experienced by a sphere in a nominally uniform mean stream (Wang & Lauchle 1999; Howe *et al.* 2001).

Figure 1 indicates how we intend to model these interactions. The impinging streamwise vortex is imagined to be contained within a randomly distorted circular cylindrical envelope of radius $R \sim \frac{1}{2}D$ impinging on the leading edge of the shroud. The envelope is broken up into a succession of statistically independent vortex structures each of which is modelled by a vortex ring of radius R. Each ring involves a distribution of spanwise vorticity of zero mean whose interaction with the airfoil is taken to be representative of the unsteady lift fluctuations. The induced motion outside the envelope consists of a steady rotational flow produced by the mean component of streamwise vorticity together with fluctuations produced by the vortex rings. The mean streamwise vorticity produces no lift on the shroud; the ring vortices generate a succession of time-dependent lift profiles that collectively determine the lift spectrum. The idealized model cannot be expected to provide an accurate representation of the actual flow, but will arguably yield statistical properties of the unsteady lift that are consistent with observations, thereby confirming the important role played by discrete vortex structures in determining the overall lift spectrum.

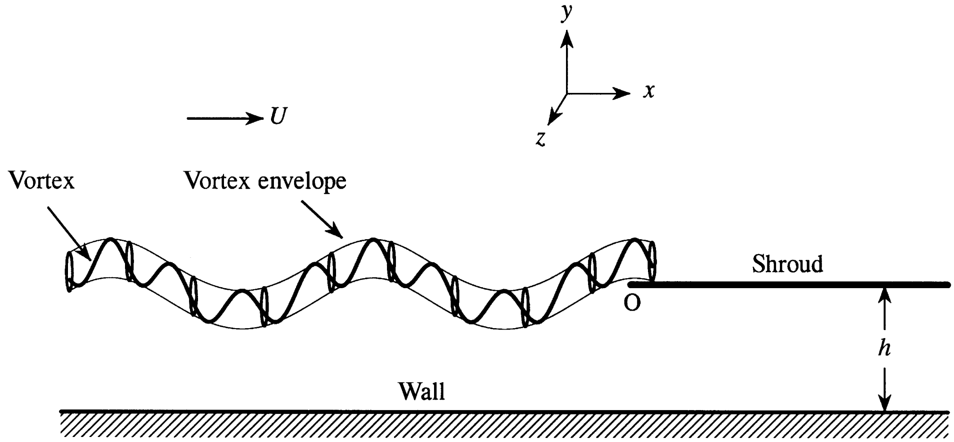

Figure 1. The impinging streamwise vortex is imagined to be contained within a randomly distorted circular cylindrical envelope of radius R that impinges on the leading edge of the shroud. The vortex is broken up into a succession of statistically independent vortex structures each of which is modelled by a ring vortex contained within the envelope and also of radius R. The vortex ring axes are taken to be parallel to the mean stream direction, i.e., the x-axis.

The formula for the lift produced by each ring is derived in Section 2. The lift spectrum is calculated in Section 3 and typical numerical predictions are illustrated in Section 4. Our results predict a broadband spectrum cut off at the higher frequencies when the hydrodynamic length scale is smaller than the vortex core diameter.

2. CALCULATION OF THE UNSTEADY LIFT

2.1. Formula for the Lift

The vortex rings are orientated with their axes in the mean stream direction, which is taken to coincide with the x-axis of the rectangular coordinates (x, y, z). The shroud is modelled by a thin, rigid strip of chord $2a$ occupying the region $0<x<2a$, $y=0$, $-\infty<z<\infty$, where the z-axis is directed along the span, transverse to the mean flow direction, and out of the plane of the paper in Figure 1. The shroud is at a fixed distance from a plane wall at $y=-h$ that can be taken to represent the neighboring casing of a turbomachine. Our results are applicable to a "free" airfoil by taking the limit $h\to\infty$. The coordinate origin is at O on the shroud leading edge defined by its intersection with the vertical plane containing the rectilinear axis of the *undisturbed* streamwise vortex; this axis is assumed to coincide with the mean position of the curvilinear axis of the vortex envelope.

Each vortex ring is taken to have constant circulation Γ and radius R which is small compared to the chord $2a$ of the shroud. During the interaction with the shroud, the rings are assumed to translate *without distortion* in the mean stream direction at a constant convection velocity U_c, equal to some prescribed fraction of the free stream speed U. This is the usual "frozen" approximation of thin airfoil theory (Howe 1998), and is expected to be valid provided $U_cR/\Gamma\gg 1$, i.e., when the convection velocity U_c is much larger than the characteristic velocity Γ/R of the motion induced by the vortex [cf. Marshall & Krishnamoorthy (1997)]. Note, however, that small and localized distortions of the vortex produced by the interaction will tend to propagate as wave-like disturbances along the vortex axis at speed $\sim\Gamma/R_c$ (Kelvin 1880; Lundgren & Ashurst 1989) where $R_c\ll R$ is the radius of the vortex core. This implies that the frozen approximation is strictly applicable

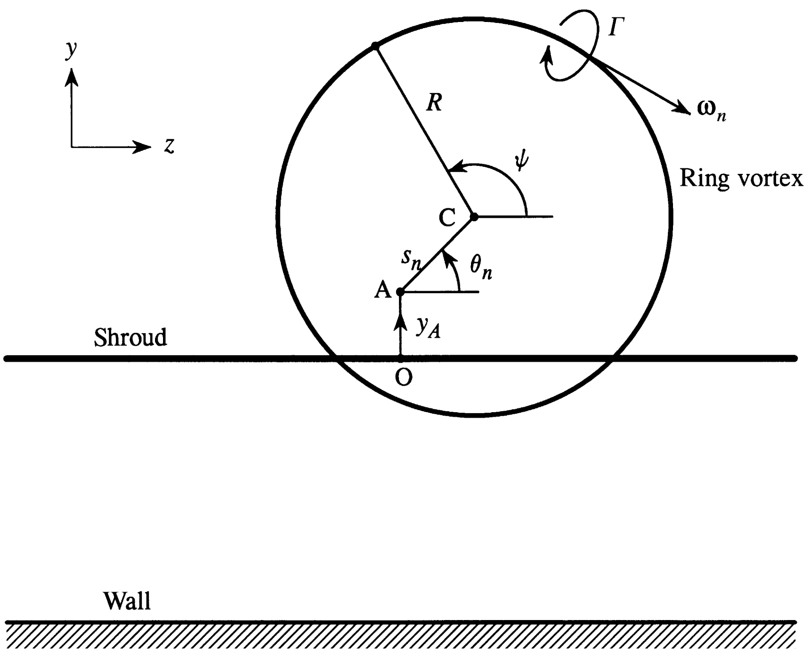

Figure 2. Streamwise view from upstream of the shroud illustrating the definition of the polar coordinates (s_n, θ_n) specifying the offset of the nth vortex ring from the undisturbed axis A of the streamwise vortex. The local coordinates (R, ψ) are used to evaluate the unsteady lift integral.

only for the more stringent condition $U_c R_c/\Gamma \gg 1$. However, these small-scale motions will be ignored. They correspond to small amplitude components of the overall motion that are significant only at high frequencies of order U_c/R_c (whereas it will be shown below that the spectrum of the lift fluctuations is dominated by components of much lower frequency $\sim U_c/R$) and are unlikely to be a correct representation of the small-scale motions occurring in the real vortex-edge interaction. We shall similarly ignore the high-frequency contributions from the small additional vorticity associated with a possible *velocity defect* in the cores of the vortex rings.

The undisturbed axis of the streamwise vortex lies along the straight line $x = 0$, $y = y_A$, and is denoted by A in Figure 2, where the view is in the x-direction from upstream of the leading edge of the shroud. Center C of the nth ring is offset from A distance s_n in a direction making an angle θ_n with the positive z-axis. The azimuthal vorticity $\boldsymbol{\omega}_n$ is in the clockwise direction in Figure 2. The plane of the nth ring is cut by the leading edge of the shroud at time $t = t_n$. If $R > |y_A + s_n \sin\theta_n|$, the vortex ring is also cut by the shroud. When this happens it is assumed that during the brief interval in which the unsteady lift force is significant, i.e., while the plane of the vortex is within a distance of order R from the edge, both sections of the severed vortex continue to convect parallel to the shroud at velocity U_c.

At small mean flow Mach numbers, the local flow can be regarded as incompressible, and the unsteady lift (in the $+y$-direction) on the shroud can be calculated from the incompressible flow formula (Howe 1998, 2001)

$$\mathscr{L}(t) = \rho_o \int \nabla X_2 \cdot \boldsymbol{\omega} \wedge \mathbf{v}\, \mathrm{d}^3\mathbf{x} - \eta \oint_S \boldsymbol{\omega} \wedge \nabla \boldsymbol{X}_2 \cdot \mathrm{d}\mathbf{S}, \tag{2.1}$$

where ρ_o, η are, respectively, the mean density and shear viscosity of the fluid, $\mathbf{v}(\mathbf{x}, t)$ is the fluid velocity, and $\boldsymbol{\omega} \equiv \text{curl } \mathbf{v}$ is the vorticity. The integrations are taken, respectively, over the vortical regions of the flow and over the surface of the shroud (where the vector surface element $\mathrm{d}\mathbf{S}$ is directed into the fluid). The function $X_2 \equiv X_2(\boldsymbol{x})$ is a solution of Laplace's equation [determined in Howe (2001)] in the region $x_2 > -h$ above the wall satisfying $\partial X_2/\partial x_2 = 1$ on $x_2 = -h$ and having vanishing normal derivative on the shroud. The surface integral represents the frictional component of the force and will be discarded, since its contribution at high Reynolds numbers is small.

The dominant interactions between a ring vortex and the shroud occur at the leading and trailing edges. Additional vorticity is produced by these interactions at the trailing edge and shed into the wake. However, when the vortex radius R is much smaller than the chord $2a$ of the shroud, the characteristic *reduced frequency* of shedding $\omega a/U \sim a/R \gg 1$ and the length scale of the wake vorticity $\sim U/\omega \ll a$. Vortex shedding then has a negligible influence on the interaction between the ring and the leading edge; most of the shedding occurs as the vortex passes the trailing edge. When $\omega a/U \gg 1$, the shed vorticity produces an unsteady contribution to the lift that is essentially equal and opposite in sign to that generated by the vortex ring *interacting with the trailing edge* (Howe 1998). The contribution from the wake to the vorticity $\boldsymbol{\omega}$ in equation (2.1) can therefore be discarded provided the lift generated by the interaction of the vortex ring with the trailing edge is also neglected. Because $R \ll 2a$, we can do this by expanding the function $X_2(\mathbf{x})$ in equation (2.1) about the leading edge at $x = 0$, $y = 0$ [a procedure that has been justified at high reduced frequencies by Howe (2001)].

The leading order term in this expansion is [details are given by Howe (2001)]

$$\begin{aligned} X_2 &\approx f\left(\frac{a}{h}\right) \mathscr{R}e\left\{\sqrt{2a}\sqrt{x + \mathrm{i}y}\right\} \\ &= f\left(\frac{a}{h}\right)\sqrt{2a}(x^2 + y^2)^{1/4} \cos\left(\frac{\vartheta}{2}\right), \quad 0 < \vartheta < 2\pi, \quad -\infty < z < \infty, \end{aligned} \tag{2.2}$$

where $(x, y) = (x^2 + y^2)^{1/2}(\cos\vartheta, \sin\vartheta)$, and where $f(a/h)$ is a monotonically increasing function of the ratio a/h of the shroud semi-chord to the clearance h between the shroud and the wall. The function $f(a/h) \sim (a/\pi h)^{1/2}$ as $a/h \to \infty$, and it is well approximated by

$$f\left(\frac{a}{h}\right) \approx \frac{1}{\sqrt{2}}\left[1 + \left(1 + \frac{(a/h)^2}{1 + 0{\cdot}13(a/h) - 0{\cdot}0045(a/h)^2}\right)^{1/2}\right]^{1/2} \quad \text{for } 0 \leqslant \frac{a}{h} \leqslant 10. \tag{2.3}$$

If $\mathscr{L}_n(t - t_n)$ is the lift attributable to the nth vortex, the net lift becomes

$$\mathscr{L}(t) = \sum_{n=-\infty}^{\infty} \mathscr{L}_n(t - t_n), \tag{2.4}$$

where

$$\mathscr{L}_n(t - t_n) = \rho_o \int \nabla X_2 \cdot \boldsymbol{\omega}_n \wedge \mathbf{v}\, \mathrm{d}^3\mathbf{x} \tag{2.5}$$

and $\boldsymbol{\omega}_n(\mathbf{x}, t)$ is the vorticity distribution of the nth vortex ring, which crosses the leading edge of the shroud at time $t = t_n$.

To evaluate the integral, the cross-section of the vortex core will initially be regarded as infinitesimal. If r denotes perpendicular distance from the axis A of the nth vortex in the direction of the unit vector $\hat{\mathbf{r}}$, then

$$\boldsymbol{\omega}_n \wedge \mathbf{v} = U_c \Gamma \delta(r - R)\delta(x - U_c(t - t_n))\hat{\mathbf{r}} \tag{2.6}$$

and therefore

$$\mathscr{L}_n(t - t_n) = \rho_o U_c \Gamma f\left(\frac{a}{h}\right)\left(\frac{aR}{2}\right)^{1/2} \mathscr{F}_n(t - t_n), \tag{2.7}$$

where

$$\mathscr{F}_n(t - t_n) = \mathscr{R}e \int_0^{2\pi} \frac{\mathrm{i}\sin\psi\,\mathrm{d}\psi}{\sqrt{U_c(t - t_n)/R + \mathrm{i}\big(y_A/R + (s_n/R)\sin\theta_n + \sin\psi\big)}}, \tag{2.8}$$

and ψ is the angle shown in Figure 2. The branch of the complex square root is defined as in equation (2.2), with the argument ϑ confined to the interval $0 < \vartheta < 2\pi$. If $|y_A + s_n \sin\theta_n| < R$ the vortex ring is cut by the leading edge at $t = t_n$, and the integrand is then discontinuous for $t > t_n$ where $\sin\psi = -(y_A + s_n \sin\theta_n)/R$.

2.2. Lift Generated by a Single Vortex Ring

The integral equation (2.8) can be evaluated numerically for each vortex ring. The plots in Figure 3 illustrate the time dependence of the nondimensional lift

$$\mathscr{L}_n(t - t_n)/\rho_o U_c \Gamma f\left(\frac{a}{h}\right)\left(\frac{aR}{2}\right)^{1/2}.$$

This nondimensional ratio is independent of the chord $2a$ of the shroud, because of our assumption that $R \ll a$. The lift profiles are plotted for

$$\frac{d}{R} \equiv \frac{y_A}{R} + \frac{s_n}{R}\sin\theta_n = 0.5,\ \ 0.9,\ \ 1.4.$$

When $d < R$ the vortex is severed at $t = t_n$; the corresponding lift profiles shown in the figure (for $d/R = 0.5,\ 0.9$) exhibit a discontinuous change in slope at this time. The slope is finite for $t < t_n$, but

$$\frac{\mathrm{d}\mathscr{L}_n}{\mathrm{d}t} \sim \rho_o U_c \Gamma f\left(\frac{a}{h}\right)\left(\frac{aR}{2}\right)^{1/2} \frac{4d}{\sqrt{R^2 - d^2}} \sqrt{\frac{U_c/R}{t - t_n}} \quad \text{as } t \to t_n + 0, \quad 0 < d < R$$

and the magnitude of the lift assumes a sharp maximum at $t = t_n$. The lift becomes singular at $d = R$, because of the neglect of the finite core size of the vortex; this is discussed in Section 4. When $d > R$, the vortex does not make contact with the leading edge of the shroud, and the lift profile is always smooth, decaying to zero very rapidly with increasing values of d/R.

The results shown in Figure 3 are for situations where the center of the vortex always passes above the shroud. When $d < 0$, the lift profiles are the same as for positive values of d but reversed in sign. In particular, the lift vanishes identically for all times when $d = 0$ and the vortex is bisected by the shroud. In all cases, the net variation in the unsteady lift occurs during the time in which the center of the vortex is within a distance of about $2R$ from the leading edge.

3. THE LIFT SPECTRUM

3.1. The Mean Lift

The quasi-periodic impingement of vortex rings on the leading edge of the shroud implies the existence of a mean period τ, say, between the successive arrivals of vortices at the

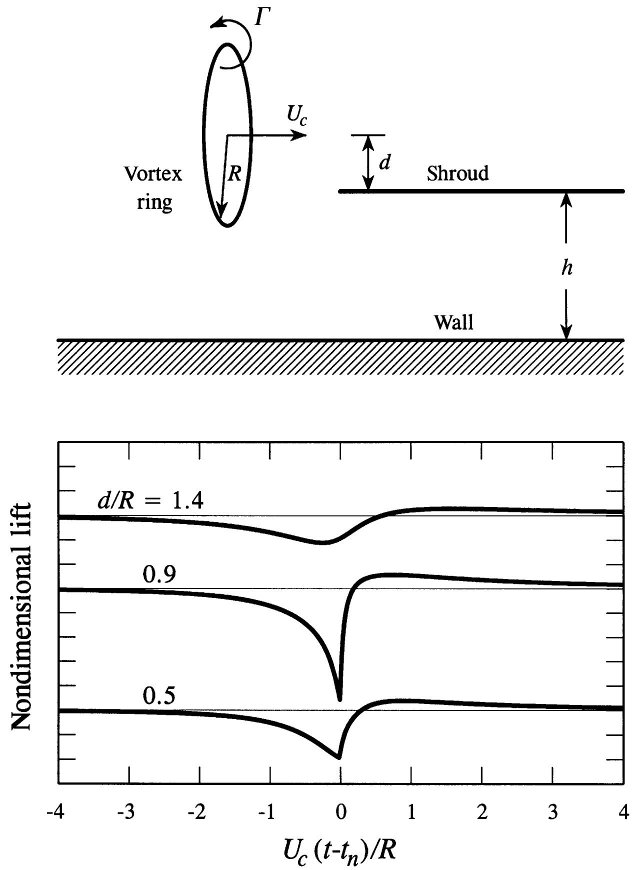

Figure 3. Variation of the nondimensional lift produced by the nth vortex $\mathscr{L}_n(t-t_n)/\rho_o U_c \Gamma f(a/h)(aR/2)^{1/2}$, for $d/R = 0{\cdot}5,\ 0{\cdot}9,\ 1{\cdot}4$.

edge. This mean period defines a characteristic frequency

$$f_o = \frac{1}{\tau} \tag{3.1}$$

determined, in practice, by vortex shedding at an upstream station occurring at a characteristic value of the Strouhal number $f_0 D/U$.

The time-dependent lift is given by

$$\mathscr{L}(t) = \rho_o U_c \Gamma f\left(\frac{a}{h}\right)\left(\frac{aR}{2}\right)^{1/2} \sum_n \mathscr{F}_n(t-t_n). \tag{3.2}$$

The mean lift does not vanish unless the vertical offset y_A of the mean axis of the streamwise vortex also vanishes. The *ensemble average* mean lift is found by averaging with respect to the vortex configuration parameters s_n, θ_n, and is written as

$$\langle \mathscr{L}(t) \rangle = \rho_o U_c \Gamma f\left(\frac{a}{h}\right)\left(\frac{aR}{2}\right)^{1/2} \sum_n \langle \mathscr{F}_n(t-t_n) \rangle, \tag{3.3}$$

where the angle brackets denote the ensemble average.

Let

$$\hat{\mathscr{F}}_n(\omega) = \frac{1}{2\pi}\int_{-\infty}^{\infty} \mathscr{F}_n(t)\mathrm{e}^{\mathrm{i}\omega t}\,\mathrm{d}t \tag{3.4}$$

be the Fourier transform of $\mathscr{F}_n(t)$. Then,

$$\langle \mathscr{L}(t)\rangle = \rho_o U_c \Gamma f\left(\frac{a}{h}\right)\left(\frac{aR}{2}\right)^{1/2}\int_{-\infty}^{\infty}\sum_n \langle \hat{\mathscr{F}}_n(\omega)\rangle \mathrm{e}^{-\mathrm{i}\omega(t-n\tau)}\,\mathrm{d}\omega. \tag{3.5}$$

The ensemble average $\langle \hat{\mathscr{F}}_n(\omega)\rangle$ is independent of n. Thus, if equation (3.5) is next averaged over a large time interval $-T<t<T$ ($T \gg \tau$) and account is taken of the formula (Lighthill 1958)

$$\frac{\sin(\omega T)}{\omega} \to \pi\delta(\omega) \quad \text{as} \quad T \to \infty, \tag{3.6}$$

the time-averaged *mean lift* $\overline{\mathscr{L}}$ is found to be

$$\overline{\mathscr{L}} = \frac{\pi\rho_o U_c \Gamma}{T} f\left(\frac{a}{h}\right)\left(\frac{aR}{2}\right)^{1/2}\sum_n{}' \langle \hat{\mathscr{F}}_n(0)\rangle, \tag{3.7}$$

where the prime indicates that the summation is confined to those vortices that interact with the leading edge of the shroud during $-T<t<T$. When $T \gg \tau$, there are approximately $2T/\tau$ such interactions, and the mean lift therefore becomes

$$\overline{\mathscr{L}} = \frac{2\pi\rho_o U_c \Gamma}{\tau} f\left(\frac{a}{h}\right)\left(\frac{aR}{2}\right)^{1/2}\langle \hat{\mathscr{F}}_n(0)\rangle \equiv \frac{\rho_o U_c \Gamma}{\tau} f\left(\frac{a}{h}\right)\left(\frac{aR}{2}\right)^{1/2}\int_{-\infty}^{\infty}\langle \mathscr{F}_n(t)\rangle\,\mathrm{d}t. \tag{3.8}$$

The integral can be evaluated for each vortex, and the average taken over an ensemble of values of s_n and θ_n. In principle, this formula could be used to estimate, say, the value of the vortex circulation Γ by equating $\overline{\mathscr{L}}$ to an observed mean lift.

3.2. The Unsteady Lift

Consider the unsteady lift

$$\begin{aligned}\mathscr{L}'(t) &= \mathscr{L}(t) - \langle \mathscr{L}\rangle \\ &= \rho_o U_c \Gamma f\left(\frac{a}{h}\right)\left(\frac{aR}{2}\right)^{1/2}\sum_n (\mathscr{F}_n(t-t_n) - \langle \mathscr{F}_n(t-t_n)\rangle).\end{aligned} \tag{3.9}$$

When successive vortex rings are statistically independent, the ensemble average square unsteady lift is

$$\langle \mathscr{L}'^2(t)\rangle = \left[\rho_o U_c \Gamma f\left(\frac{a}{h}\right)\left(\frac{aR}{2}\right)^{1/2}\right]^2 \sum_n \left\langle (\mathscr{F}_n(t-t_n) - \langle \mathscr{F}_n(t-t_n)\rangle)^2\right\rangle. \tag{3.10}$$

In terms of the Fourier transform defined in equation (3.4), this is equivalent to

$$\begin{aligned}\langle \mathscr{L}'^2(t)\rangle = \left[\rho_o U_c \Gamma f\left(\frac{a}{h}\right)\left(\frac{aR}{2}\right)^{1/2}\right]^2 \int\int_{-\infty}^{\infty}\sum_n \Big\langle \big(\hat{\mathscr{F}}_n(\omega) \\ - \langle \hat{\mathscr{F}}_n(\omega)\rangle\big)\big(\hat{\mathscr{F}}_n^*(\omega') - \langle \hat{\mathscr{F}}_n^*(\omega')\rangle\big)\Big\rangle \mathrm{e}^{-\mathrm{i}(\omega-\omega')(t-n\tau)}\,\mathrm{d}\omega\,\mathrm{d}\omega',\end{aligned} \tag{3.11}$$

where the asterisk denotes complex conjugate. As before, the ensemble average in the integrand does not depend on n, so that by averaging with respect to time and using formula (3.6) with ω replaced by $\omega - \omega'$, the mean square fluctuating lift is rendered in the form

$$\overline{\mathscr{L}'^2} = \frac{2\pi}{\tau}\left[\rho_o U_c \Gamma f\left(\frac{a}{h}\right)\left(\frac{aR}{2}\right)^{1/2}\right]^2 \int_{-\infty}^{\infty} \left\{\left\langle|\hat{\mathscr{F}}_n(\omega)|^2\right\rangle - |\langle\hat{\mathscr{F}}_n(\omega)\rangle|^2\right\} \mathrm{d}\omega. \tag{3.12}$$

Hence, if the frequency spectrum $\Phi(\omega)$ of the unsteady lift is defined by

$$\overline{\mathscr{L}'^2} = \int_{-\infty}^{\infty} \Phi(\omega)\,\mathrm{d}\omega, \tag{3.13}$$

we have

$$\Phi(\omega) = \frac{2\pi}{\tau}\left[\rho_o U_c \Gamma f\left(\frac{a}{h}\right)\left(\frac{aR}{2}\right)^{1/2}\right]^2 \left\{\left\langle|\hat{\mathscr{F}}_n(\omega)|^2\right\rangle - |\langle\hat{\mathscr{F}}_n(\omega)\rangle|^2\right\}, \tag{3.14}$$

where the remaining averages are ensemble averages to be taken over all possible vortex ring configurations determined by the permissible values of $s_n,\ \theta_n$.

4. NUMERICAL RESULTS

4.1. The Lift Spectrum

Using definition (2.8), we readily calculate that

$$\hat{\mathscr{F}}_n(\omega) = \frac{1}{2\pi}\int_{-\infty}^{\infty} \mathscr{F}_n(t)\mathrm{e}^{\mathrm{i}\omega t}\,\mathrm{d}t = \frac{\mathrm{e}^{-(\mathrm{i}\pi/4)\mathrm{sgn}(\omega)}}{2\sqrt{\pi|\omega R/U_c|}}$$
$$\times \int_0^{2\pi} \sin\psi \exp\{-|\omega R/U_c|\left|y_A/R + (s_n/R)\sin\theta_n + \sin\psi\right|\}\,\mathrm{d}\psi. \tag{4.1}$$

This formula reveals that $\hat{\mathscr{F}}_n(\omega)$ decays exponentially fast with increasing values of $\omega R/U_c$ when $|d| = |y_A + s_n \sin\theta_n| > R$, i.e., when the vortex is *not* cut by the shroud (so that the argument of the exponential in the second integrand is nonzero for all azimuthal angles ψ). If $|y_A + s_n\sin\theta_n| < R$, then the integral is dominated as $|\omega R/U_c| \to \infty$ by values of ψ in the vicinity of the two angles, where

$$\frac{y_A}{R} + \frac{s_n}{R}\sin\theta_n + \sin\psi = 0,$$

which define the points of intersection of the vortex and the shroud. We then find

$$\hat{\mathscr{F}}_n(\omega) \sim \frac{2\mathrm{e}^{-(\mathrm{i}\pi/4)\mathrm{sgn}(\omega)}}{\pi^{1/2}|\omega R/U_c|^{3/2}}\frac{(y_A + s_n\sin\theta_n)}{\sqrt{R^2 - (y_A + s_n\sin\theta_n)^2}}, \quad \frac{\omega R}{U_c} \to \infty. \tag{4.2}$$

For finite frequencies, the ψ-integral in equation (4.1) must be evaluated numerically.

Figure 4 shows the normalized lift spectrum $10 \times \log_{10}\Phi'(\omega)$ (dB) plotted against $\omega R/U_c$, where

$$\Phi'(\omega) = \Phi(\omega)\Bigg/\frac{2\pi}{\tau}\left[\rho_o U_c \Gamma f\left(\frac{a}{h}\right)\left(\frac{aR}{2}\right)^{1/2}\right]^2 \tag{4.3}$$

for the particular case $y_A = 0$ when the axis of the undisturbed streamwise vortex lies in the plane of the shroud, and for the following *constant* values of the radial offset

$$s_n/R = 0{\cdot}5, \quad 0{\cdot}9, \quad 1{\cdot}4.$$

The mean lift vanishes when $y_A = 0$ ($\langle\hat{\mathscr{F}}_n(\omega)\rangle = 0$), and equation (3.14) gives $\Phi'(\omega) = \left\langle|\hat{\mathscr{F}}_n(\omega)|^2\right\rangle$. When s_n/R is constant, the strength of the interaction of a vortex

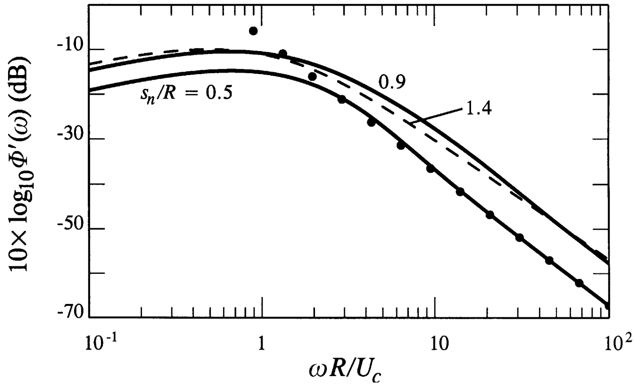

Figure 4. Nondimensional lift spectrum $10\log_{10}\Phi'(\omega)$ (dB) for $y_A = 0$ and $s_n/R = 0{\cdot}5,\ 0{\cdot}9,\ 1{\cdot}4$ averaged over 1000 realizations of the vortex ring angle θ_n, which is assumed to be uniformly distributed in $0<\theta_n<2\pi$. Also shown (•••) is the asymptotic ensemble average spectrum determined by equation (4.2) for the case $s_n/R = 0{\cdot}5$.

ring with the shroud varies with the angle θ_n. Average values have been computed from equation (4.1) using an ensemble of 1000 vortex rings and by taking θ_n to be uniformly distributed over $0<\theta_n<2\pi$. The dotted straight line in the figure represents the corresponding ensemble average obtained by using the high-frequency asymptotic approximation (4.2), which implies that $\Phi'(\omega) \sim (\omega R/U_c)^{-3}$ for $\omega R/U_c \gg 1$; this is shown only for $s_n/R = 0{\cdot}5$.

It has already been seen in Figure 3 that the maximum lift increases with $|d| = |s_n \sin\theta_n|$ provided $|d|<R$. Further increases in $|d|$ result in a smooth and gradually decreasing lift profile. In consequence, the lift spectra also increase in overall strength as s_n increases to R, following which there is a slow decay. This is reflected in the results shown in Figure 4. At $s_n/R = 1.4$, the spectrum has evidently stopped increasing, and further increases in s_n will be evidenced by an overall drop in the spectrum.

4.2. The Influence of Finite Core Size

Approximate account can be taken of the influence of the finite radius R_c, say, of the vortex core provided R_c is small compared to the vortex ring radius R. This is done by assuming the core to have circular cross-section, and by observing that the net lift can be regarded as a linear superposition of the lifts produced by coaxial, elementary ring vortices of infinitesimal core radii distributed over this core. The modification of the lift spectrum must be small when $\omega R_c/U_c$ is small. As the frequency increases, however, phase interference between the contributions to $\hat{\mathscr{F}}_n(\omega)$ from the different elementary vortices will cause the spectrum to decrease rapidly.

The modified spectrum is easily determined when the vorticity within the core has the Gaussian distribution

$$\frac{\Gamma}{\pi R_c^2}\,\mathrm{e}^{-r_\perp^2/R_c^2}, \quad R_c \ll R,$$

where $r_\perp$ denotes radial distance from the core axis. We then obtain the following modification of equation (3.14)

$$\frac{\Phi(\omega)}{(2\pi/\tau)\left[\rho_o U_c \Gamma f(a/h)(aR/2)^{1/2}\right]^2} = \left\{\left\langle|\hat{\mathscr{F}}_n(\omega)|^2\right\rangle - |\left\langle\hat{\mathscr{F}}_n(\omega)\right\}\mathrm{e}^{-(1/2)\left(\omega R_c/U_c\right)^2}. \quad (4.4)$$

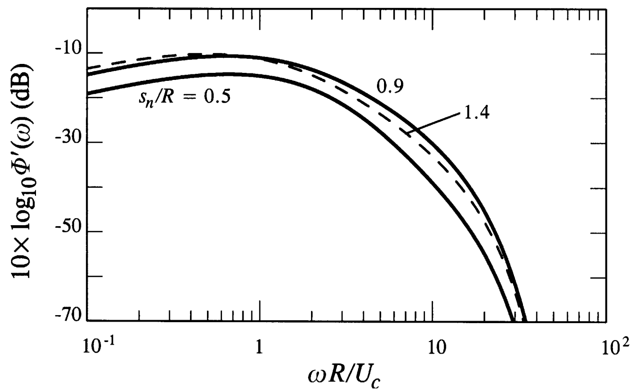

Figure 5. Nondimensional lift spectrum $10\log_{10}\Phi'(\omega)$ (dB) for $y_A = 0$ and $s_n/R = 0{\cdot}5,\ 0{\cdot}9,\ 1{\cdot}4$ averaged over 1000 realizations of the vortex ring angle θ_n uniformly distributed over $0 < \theta_n < 2\pi$, when the vortex core radius $R_c = 0{\cdot}1R$.

The effect of the correction factor $e^{-(1/2)(\omega R_c/U_c)^2}$ on the spectra of Figure 4 is shown in Figure 5 for the case $R_c = 0{\cdot}1R$. The lift decreases very rapidly when $\omega R/U_c$ exceeds about 10. For smaller frequencies, the spectrum remains relatively flat. Since, by hypothesis, the radius R of the vortex rings is much smaller than the airfoil chord $2a$, this flat spectrum will extend over a significant range of reduced frequencies $\omega a/U_c$, typically occupying in the interval $1 < \omega a/U_c < 100$.

5. CONCLUSION

A streamwise vortex "playing" on the leading edge of an airfoil usually exhibits a random wave-like instability induced by interaction with the mean flow and the upstream influence of the edge. In many cases, the vortex already contains quasi-periodic structures characterized by a Strouhal number determined by the original source of the vortex. The calculation of the resulting modulation of the airfoil lift requires a detailed knowledge of the vorticity distribution near the leading edge. We have modelled the quasi-periodic structures by a succession of uncorrelated vortex rings randomly incident on the leading edge, within a certain prescribed envelope taken to be determined by the mean flow conditions. When the vortices are assumed to convect at a mean velocity U_c, the overall lift fluctuation can be calculated as a linear superposition of the separate lifts induced by each vortex.

The quasi-periodic vortex structures induce a broad-band lift spectrum that is relatively flat up to a maximum frequency governed by the diameter of the vortex core. This region of the spectrum can typically span an interval $1 < \omega a/U < 100$ of airfoil-reduced frequencies. These general, statistical predictions are unlikely to be critically dependent on the precise details of the vortex structures, and can therefore be expected to be representative of what happens in practice.

References

Blevins, R. D. 1977 *Flow Induced Vibration*. New York: Van Nostrand Reinhold.

Canbazoglu, S., Lin, J.-C., Wolfe, S. & Rockwell, D. 1995 Buffeting of fins: distortion of incident vortex. *AIAA Journal* **33,** 2144–2150.

CURLE, N. 1955 The influence of solid boundaries upon aerodynamic sound. *Proceedings of the Royal Society of London A* **231,** 505–514.
GEBERT, G. A. & ATASSI, H. M. 1989 Unsteady vortical disturbances around a thin airfoil in the presence of a wall. *AIAA Journal* **27,** 1448–1450.
GREEN, S. I. 1995 Wing tip vortices. In *Fluid Vortices* (ed S. I. Green, Chapter X). Dordrecht: Kluwer Academic Publishers.
HOWE, M. S. 1988 Contributions to the theory of sound production by vortex–airfoil interaction, with application to vortices with finite axial velocity defect. *Proceedings of the Royal Society A* **420,** 157–182.
HOWE, M. S. 1991 On the estimation of the sound produced by complex fluid–structure interactions, with application to a vortex interacting with a shrouded rotor in a duct. *Proceedings of the Royal Society of London A* **433,** 573–598.
HOWE, M. S. 1998 *Acoustics of Fluid–Structure Interactions*. Cambridge: Cambridge University Press.
HOWE, M. S. 2001 Unsteady lift and sound produced by an airfoil in a turbulent boundary layer. *Journal of Fluids and Structures* **15,** 207–225.
HOWE, M. S., LAUCHLE, G. C. & WANG, J. 2001 Aerodynamic lift and drag fluctuations of a sphere. *Journal of Fluid Mechanics* **436,** 41–57.
KELVIN, Lord 1880 Vibrations of a columnar vortex. *Philosophical Magazine* **10,** 155–168.
LIGHTHILL, M. J. 1958 *An Introduction to Fourier Analysis and Generalised Functions*. Cambridge: Cambridge University Press.
LUNDGREN, T. S. & ASHURST, W. T. 1989 Area-varying waves on curved vortex tubes with application to vortex breakdown. *Journal of Fluid Mechanics* **200,** 283–307.
MARSHALL, J. S. & KRISHNAMOORTHY, S. 1997 On the instantaneous cutting of a columnar vortex with non-zero axial flow. *Journal of Fluid Mechanics* **351,** 41–74.
MAYORI, A. & ROCKWELL, D. 1994 Interaction of a streamwise vortex with a thin plate: a source of turbulent buffeting. *AIAA Journal* **32,** 2022–2029.
ROCKWELL, D. 1998 Vortex–body interactions. *Annual Review of Fluid Mechanics* **30,** 199–229.
SEARS, W. R. 1941 Some aspects of non-stationary airfoil theory and its practical applications. *Journal of Aeronautical Science* **8,** 104–108.
WAITZ, I. A., GREITZER, E. M. & TAN, C. S. 1995 Vortices in aero-propulsion systems. In *Fluid Vortices* (ed. S. I. Green) (Chapter XI). Dordrecht: Kluwer Academic Publishers.
WANG, J.-J. & LAUCHLE, G. C. 1999 Hydrodynamic lift and drag fluctuations of a sphere. PennState Applied Research Laboratory Report 00–005.
WITTMER, K.S. & DEVENPORT, W.J. 1999 Effects of perpendicular blade–vortex interaction. Part 1: turbulence structure and development. *AIAA Journal* **37,** 805–812.
WITTMER, K.S., DEVENPORT, W.J. & GLEGG, S.A.L. 1999 Effects of perpendicular blade–vortex interaction. Part 2: parameter study. *AIAA Journal* **37,** 813–817.
WITTMER, K. S., DEVENPORT, W. J., RIFE, M. C. & GLEGG, S. A. L. 1995 Perpendicular blade-vortex interaction. *AIAA Journal* **33,** 1667–1674.
WOLFE, S., LIN, J.-C. & ROCKWELL, D. 1995 Buffeting at the leading edge of a flat plate due to a streamwise vortex. *Journal of Fluids and Structures* **9,** 359–370.